

## Enhanced magnetocrystalline anisotropy in deposited cobalt clusters

This article has been downloaded from IOPscience. Please scroll down to see the full text article.

2002 J. Phys.: Condens. Matter 14 605

(<http://iopscience.iop.org/0953-8984/14/3/327>)

View [the table of contents for this issue](#), or go to the [journal homepage](#) for more

### Download details:

IP Address: 171.66.16.238

The article was downloaded on 17/05/2010 at 04:46

Please note that [terms and conditions apply](#).

# Enhanced magnetocrystalline anisotropy in deposited cobalt clusters

D A Eastham<sup>1</sup>, P M Denby<sup>1</sup>, A Harrison<sup>2</sup>, I W Kirkman<sup>1</sup> and  
A G Whittaker<sup>2</sup>

<sup>1</sup> Daresbury Laboratory, Daresbury, Warrington WA4 4AD, UK

<sup>2</sup> Department of Chemistry, University of Edinburgh, Edinburgh EH9 3JJ, UK

Received 19 July 2001, in final form 22 October 2001

Published 21 December 2001

Online at [stacks.iop.org/JPhysCM/14/605](http://stacks.iop.org/JPhysCM/14/605)

## Abstract

The magnetic properties of nanomaterials made by embedding cobalt nanocrystals in a copper matrix have been studied using a SQUID magnetometer. The remanent magnetization at temperatures down to 1.8 K and the RT (room temperature) field-dependent magnetization of 1000- and 8000-atom (average-size) cobalt cluster samples have been measured. In all cases it has been possible to relate the morphology of the material to the magnetic properties. However, it is found that the deposited cluster samples contain a majority of sintered clusters even at cobalt concentrations as low as 5% by volume. The remanent magnetization of the 8000-atom samples was found to be bimodal, consisting of one contribution from spherical particles and one from touching (sintered) clusters. Using a Monte Carlo calculation to simulate the sintering it has been possible to calculate a size distribution which fits the RT superparamagnetic behaviour of the 1000-atom samples. The remanent magnetization for this average size of clusters could then be fitted to a simple model assuming that all the nanoparticles are spherical and have a size distribution which fits the superparamagnetic behaviour. This gives a value for the potential energy barrier height (for reversing the spin direction) of  $2.0 \mu\text{eV}/\text{atom}$  which is almost four times the accepted value for face-centred-cubic bulk cobalt. The remanent magnetization for the spherical component of the large-cluster sample could not be fitted with a single barrier height and it is conjectured that this is because the barriers change as a function of cluster size. The average value is  $1.5 \mu\text{eV}/\text{atom}$  but presumably this value tends toward the bulk value ( $0.5 \mu\text{eV}/\text{atom}$ ) for the largest clusters in this sample.

## 1. Introduction

The morphology of deposited clusters is a subject [1] of much current interest. It has been determined in the past by using transmission electron microscopy (TEM) and nanoprobe

microscopy (STM and AFM). Two general results are obtained from previous work. The first is that there is an increase in the amount of sintering [2] during deposition above that expected from a purely random process. Indeed many studies [3,4] show the growth of islands for small clusters or dendritic growth for larger ones. This is thought to be due to surface motion (diffusion) on impact, and simple models [2,5] of this behaviour have been proposed. It is possible however to obtain isolated cluster assemblies [6–9] if the deposition energy is low enough and the coverage is small. Recent experiments with size-selected, soft-landed gold clusters [10] show that it is also possible to obtain isolated (nanocrystalline) clusters on surfaces at relative coverages of 5% or more and with a narrow size distribution identical to that emitted from the cluster source. This occurs on certain substrates if the cluster beam energy and angular divergence are sufficiently small and the size is greater than about 5 nm. For small gold clusters (around 3 nm in size) the size distribution is only the same as the source distribution for very low densities. At higher densities the surface diffusion results in the formation of larger-sized clusters with masses given by multiples of the selected source mass. Furthermore, it has been found in these experiments and elsewhere [2] that small clusters usually reform into larger spherical ones when sintered. The critical size is dependent on several factors [2, 11] but appears to be about 2000 atoms for this study. Larger clusters sinter into distorted non-spherical assemblies formed from clusters fused at crystal surfaces. This difference may have several origins. Firstly, smaller clusters at the same deposition energy are more likely to melt on deposition and the fusion of two ‘liquid’ clusters is much more likely to result in a single cluster. Secondly, the surface energy term is a much larger fraction for small clusters and there is therefore a much stronger tendency to assume an overall spherical shape.

The main aim of this work was therefore to understand the magnet behaviour of nanomaterials made by this new technique. Since it was not possible to measure directly the morphology in the sample, we have calculated this from the deposited nanoparticle size distribution using knowledge of the processes which occur when clusters are deposited on surfaces. In particular we have used the remanent magnetization of large clusters to discover the degree of sintering in the deposition process and have then utilized this to compute the expected room temperature field-dependent magnetization of smaller cobalt clusters in the size range from 1000 to 3000 atoms. The calculated size distribution which was found to fit this superparamagnetic behaviour was then used to extract fundamental properties of the magnetic anisotropy of small spherical cobalt nanoparticles containing from 1000 to 3000 atoms.

## 2. Nanomaterial preparation

The nanomaterial used in these experiments was made by simultaneous deposition of clusters and atoms, so the situation is somewhat different to the studies indicated previously. However, one can surmise that the deposition and diffusion for any one cluster takes place in a time which is small compared to the time taken for the overall surface morphology to change. Thus the tendency for sintering might be similar to that of deposition of clusters alone (without the atomic beam which produces the matrix of the nanomaterial) but the growth of the ‘islands’ will be three dimensional. (Evidence supporting this conjecture is provided by the studies of the residual magnetism for large clusters when the magnetizing field is applied at different directions to the substrate.) The samples used for the work described here were made by co-depositing a cobalt cluster beam and atomic copper [12]. They were approximately 0.25  $\mu\text{m}$  thick and were capped with 15 atomic layers of copper to prevent any surface oxidation. It was therefore not possible to determine the exact morphology of the material by direct microscopy techniques. The deposited cluster sizes were determined by time-of-flight (TOF) analysis as described in [22]. Each size distribution could be fitted to a log-normal function from which it

was possible to extract the most probable size, the mean size and the FWHM of the distribution. The smaller-cluster samples had a mean size of about 1100 atoms (FWHM = 1300 atoms) and the larger-cluster samples had a mean size of about 8000 atoms (FWHM = 6000 atoms). Before each sample was made the mass distribution was measured and then fitted to a log-normal form. The precise values of the cluster size variance and most probable size were then used to compute the magnetic properties.

### 3. Measurements and analysis

Two types of measurement were made using a Quantum Design SQUID magnetometer. The first was the room temperature field-dependent magnetization. Although the remanent magnetization of the larger-cluster samples was small at RT (less than about 0.1 of the saturation magnetization), we have not tried to fit the data to the measured response because there may be significant departures [13] from the Langevin theory. For the smaller sample it is assumed that the response can be obtained by integrating [14] a convolution of the Langevin function and the size distribution.

The remanent magnetization was measured down to temperatures of 2.8 K in the following way. The sample was first cooled to the minimum temperature in a magnetic field of 1 T. The field was then reduced to zero in about 100 s and the magnetization was measured. The field was reapplied in the same direction and the sample warmed to a higher temperature. At the higher temperature the magnetization was then measured when the field was reduced to zero again in a time of about 100 s. At all stages the direction of the field was not reversed. Under these circumstances the remanent magnetization is only dependent on the sizes of the particles which are free to flip by thermal excitations when the field is reduced to zero. Thus it is not necessary to have knowledge of the fully blocked sizes, and the residual magnetization (for no cluster-cluster interactions) can be written [15] as

$$\frac{M_R}{M_S} = \frac{C \int_{N_B}^{\infty} f(N) N dN}{\int_0^{\infty} f(N) N dN} \quad (1)$$

where  $M_R$  is the residual magnetization,  $M_S$  is the saturation magnetization and  $f(N)$  is the normalized size distribution as a function of the number of atoms,  $N$ , in the cluster. The remanent magnetism thus depends critically on the blocked size,  $N_B$ , which is calculated from the dynamics of a dipole in an 'effective' internal cluster field (which creates the magnetic anisotropy) and the applied field. The constant  $C$  represents the ratio of the total dipole moment of an ensemble of clusters with randomly distributed crystal axes (in one hemisphere whose symmetry axis is the field direction) to that where the magnetization is along the magnetic field direction. It is 0.5 for a uniaxial system and 0.82 for FCC (triaxial) cobalt. We have taken the simple Néel equation [16]

$$1/\tau = f_0 \exp(-\Delta E/kT) \quad (2)$$

to describe the relaxation time  $\tau$  in terms of the potential energy barrier  $\Delta E$ . A reasonable value of the constant  $f_0$  is  $10^9 \text{ s}^{-1}$  and if the energy barriers scale directly with the cluster size, then  $\Delta E = N\varepsilon$ , where  $\varepsilon$  is the barrier height per cobalt atom. Note that  $\varepsilon$  is not the anisotropy energy density but is directly related to it [15]. A suitable choice [15] for the relaxation time is 100 s and our measurements were made in times close to this value. Using the previous equation, the blocking size is then linearly related to the temperature and this can then be used for the lower limit of the integral in equation (1) to make it possible to compute the remanent magnetism. It is easy to see from equation (2) that the blocking size is insensitive to quite large variations in the relaxation time. For this reason we have chosen not to use more exact forms for the relaxation time [17], particularly as many cannot be expressed analytically.

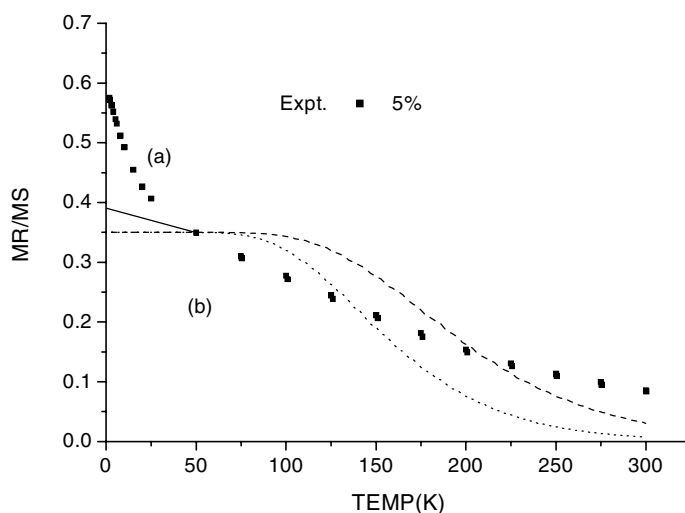


**Figure 1.** The remanent magnetization, as a fraction of the saturation magnetism (' $M_R/M_S$ '), plotted as a function of temperature. The curve can be separated into two components, one from spherical clusters (a) and one from sintered (distorted) clusters (b). The latter have a much larger anisotropy.

#### 4. Results and discussion

The remanent magnetization for 8000-atom samples at 5% volume concentration is shown in figure 1. This is clearly bimodal and the two components can be separated quite simply assuming that the value for  $M_R/M_S$ , at  $T = 0$ , is 0.5 (uniaxial) for the sintered particles and 0.82 (triaxial) for the spherical particles. (This separation was carried out by extracting the remanent magnetization at zero temperature for the two components.) It shows that 76% of the particles are sintered and have large shape (or surface) anisotropy. It should be noted that it is not possible to separate the two components in a consistent way unless the smaller component is triaxial and has  $M_R/M_S = 0.82$ . However, it is also clear that there is no single value for the anisotropy for the distorted particles. This is to be expected since there will necessarily be a range of sintered shapes. A predicted response for two values of the potential energy barrier,  $\varepsilon$ , is shown in the figure. Also we observed no difference in the response between the residual magnetization measured in the substrate plane to that measured at an angle of  $\pi/2$ . This indicates that surface diffusion, as discussed earlier, is the most likely candidate for producing the enhanced sintering.

The size distribution used to predict the RT field-dependent magnetization and the remanent magnetization for the 1000-atom samples was calculated in the following way.

Firstly a Monte Carlo simulation was used to determine the form of the size distribution for two- and three-sintered-particle clusters by randomly selecting pairs and triples from the initial distribution with a probability determined by the log-normal distribution. The fraction of double and paired particles in the final distribution was then estimated by noting that the total number of sintered particles (76%) should be the same in the large- and small-cluster samples if the surface diffusion effects were the same. We then calculated the remanent magnetization using two different ratios for the number of double and triple particles; one where the ratio is the same as for random head-on collisions (63% doubles and 13% triples) and one where the number of triples was increased to 21%.

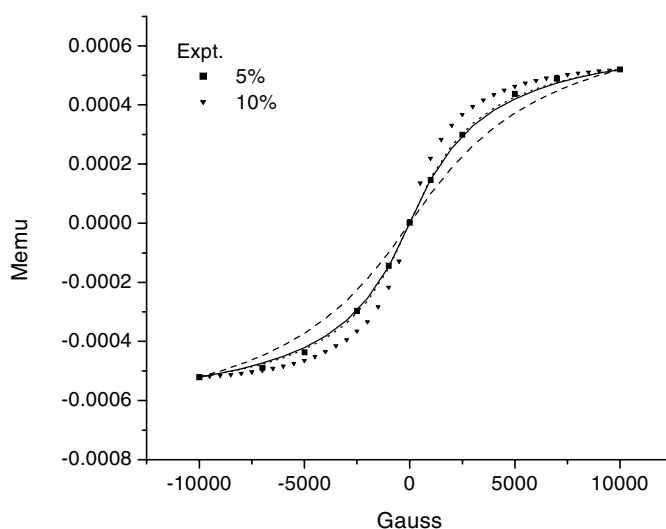


**Figure 2.** The RT field-dependent magnetization as a function of applied field for deposited clusters of average size 1000 atoms at 5 and 10% concentration. The data are compared with a convolution of the size distribution and the Langevin function. The dashed curve was obtained using the deposited size distribution and the solid curve was obtained using the size distribution modified to allow for sintered particles consisting of 63% double and 13% triple particles. The dotted curve is for 55% doubles and 21% triples.

It should be noted that this process will only produce an approximate distribution since it is quite likely that the ‘extra’ sintering probably favours larger groups of clusters more than a pure random ‘sintering-on-impact’ process where there is no diffusion of clusters. (Clearly there is diffusive sintering but it is not possible to calculate how this is distributed among 2, 3, 4, . . . groups.) The measured superparamagnetism for samples containing 5% and 10% by volume of clusters is compared with that calculated using this particle size distributions in figure 2. In this calculation we have taken a reasonable value [18] of  $1.8 \mu_B$  for the atomic moment but the fit is not altered a great deal for a value in the range from 1.6 to  $2.0 \mu_B$ . It is clear that the data cannot be understood unless extensive sintering occurs such that the average size in the sintered distribution is about double that in the cluster beam. Considering that there are no free variables, the fit is rather good and the discrepancy appears to be a failure to include enough particles smaller than the mean value since the deviations occur in the high-field region. If the number of sintered triple particles is increased to 21% the fit is only marginally better and increasing the number of larger particles even further makes the fit at low field values worse. We also show the measured values for a sample containing 10% clusters. In this sample the sintering is clearly much more severe and we cannot make any estimate of the size distribution.

The measured remanent magnetization for the 1000-atom samples is shown in figure 3, and compared to that calculated with the two size distributions used to fit the superparamagnetism. The calculated curve fits the data for the 5% sample reasonably well especially since the steeply rising part of the curve is due to clusters around the median size and this size of nanoparticle also accounts for the slope of the superparamagnetic response at fields up to 0.6 T. The tail of the distribution can be fitted reasonably well if both the number of triples is increased to 20% and the energy barriers for these particles are increased to  $3.0 \mu\text{eV}/\text{atom}$ . Whilst the latter might be plausible it cannot be considered a definite explanation of this tail without further separate information for the distribution of large particles in the sample. There is

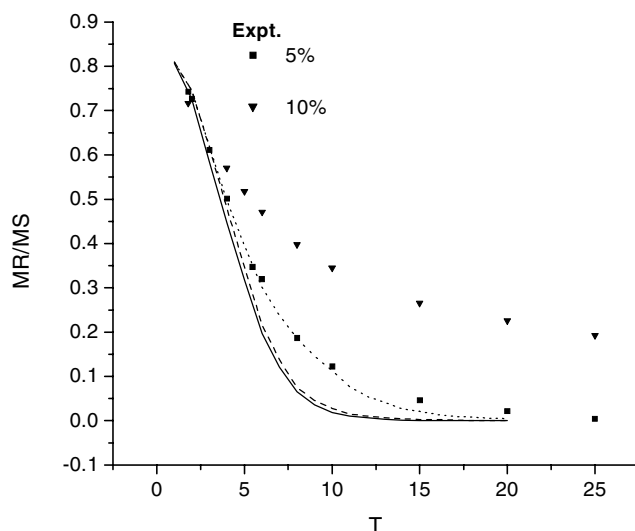


**Figure 3.** The residual magnetization as a function of the saturation magnetization for embedded cobalt clusters at 5 and 10% volume concentration. The data have been scaled by the factor 1.327 so as to get the best fit to the theory for 5% concentration. The solid curve is the theory for 63% doubles, 13% triples and the dashed curve is for 55% doubles and 21% triples, both with  $\varepsilon = 2.0 \mu\text{eV}/\text{atom}$ . The dotted curve is for 55% doubles and 21% triples but with  $\varepsilon = 3.0 \mu\text{eV}/\text{atom}$  for the tripled particles.

however a puzzling feature in the data, namely that the asymptotic measured value ( $T \rightarrow 0$ ) does not approach 0.82 but is closer to the value 0.6. A possible explanation is suggested by measurements [19] of the orbital moments in the same cluster samples. There is evidence in these measurements of changes in the orbital moment as a function of the applied field. At low fields the spin at the surface is normal to the surface whilst at higher fields (greater than about 0.5 T) it becomes parallel to the field. This implies that the total spin of the cluster increases with applied field and this change is similar to that needed to account for the decrease in the remanent magnetism found here. It is obvious that further experiments are needed to confirm this interesting hypothesis. However, it is clear that the curve predicted by equation (1) with (constant) energy barriers of  $2.0 \mu\text{eV}/\text{atom}$  is close to that measured. We have also examined the possibility that the form of the measured remanent magnetization may be in part determined by the cluster–cluster dipole interactions. The calculated average dipole–dipole interaction is of order  $0.23 \mu\text{eV}/\text{atom}$ , so this small value coupled with the fact that the sintering process depletes an area around each cluster means that this is improbable even though the dipole interaction is long range. Also it seems most unlikely that the same size distribution would fit the RT hysteresis since the dipole–dipole interactions are at least two orders of magnitude smaller than the dipole energy  $\mu \cdot H$  for all fields above 0.1 T. In other words the cluster–cluster interactions are far too weak to affect the superparamagnetism and it is therefore a realistic procedure to use a size distribution that fits the superparamagnetism to calculate the remanent magnetization. The degree of sintering in the 10% samples is considerably greater as shown by the data for the field-dependent magnetization and the remanent magnetization. Indeed preliminary data at higher temperatures show that the tail on the remanent magnetization extends beyond 50 K. The origin of this is probably due to the formation of distorted particles from multiple sintering processes. This would give rise to a bimodal distribution as found for larger clusters.

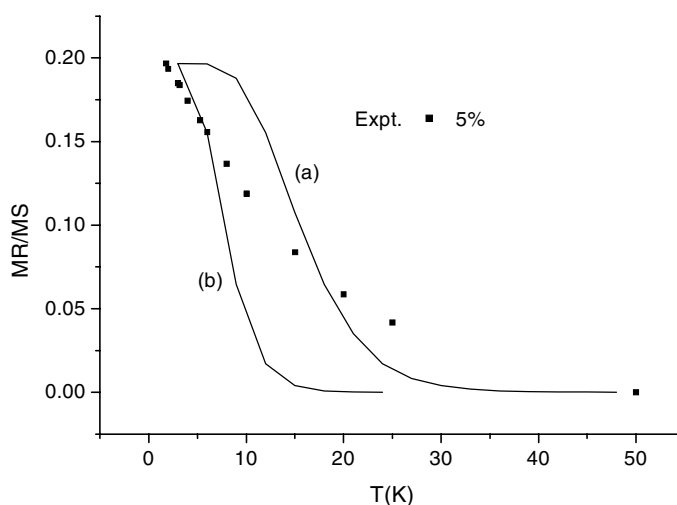


**Figure 4.** The residual magnetism for an 8000-atom average-sized cluster sample showing that it is not possible to fit the data with a single value for the energy barriers. The sintered distribution has been subtracted from the total remanent magnetization (figure 1) and the theoretical values have been calculated with the size distribution for particles in the cluster beam. (a) is for  $\varepsilon = 2.0 \mu\text{eV}/\text{atom}$  and (b) is for  $\varepsilon = 1.0 \mu\text{eV}/\text{atom}$ .

The measured value [20] of the magnetocrystalline anisotropy in bulk FCC cobalt is  $-5.86 \mu\text{eV}/\text{atom}$ , so the energy barriers [15] are  $\sim 0.5 \mu\text{eV}/\text{atom}$  which is only 1/4 of the values measured here. This is not at all surprising since small changes in the lattice dimensions can produce big changes in the magnetic anisotropy. In a nanocrystal there are necessarily quite large departures from an exact cubic structure [21] and these strains increase as the cluster size is reduced. The crystal lattice in these structures will differ significantly from that found in the bulk. It is therefore not surprising that we find an increased anisotropy. It should be noted that our measurements do not determine the sign of the anisotropy. If this is negative, as in bulk FCC cobalt, then the anisotropy is a factor of 12 times the energy barrier height and if it is positive then it is only a factor of four times the barrier height.

We might also expect the anisotropy to decrease with cluster size as the strains in the bulk of the crystal are reduced. This is evident in figure 4 which shows the spherical nanoparticle component of the remanent magnetization for the larger clusters compared with that calculated from equation (1). It is also clear that the data cannot be fitted with a single value for the energy barriers. However, it is possible to reproduce the measured value by allowing a substantial decrease in the energy barrier,  $\varepsilon$ , as a function of nanocrystal size. This was not attempted because the barrier heights become significantly less than  $1.0 \mu\text{eV}/\text{atom}$ , and at this point cluster dipole–dipole interactions are expected to contribute to the form of the residual magnetism. It is clear however that measurements on size-selected clusters are required to make further progress in this area.

## 5. Conclusions

There are therefore two overall conclusions of this work. Firstly the measurements show that cobalt clusters in the size range covered by the 1000-atom samples (1000–3000 atoms) have specific barrier heights which are fairly constant at  $2.0 \mu\text{eV}/\text{atom}$  and that these decrease



thereafter with increasing cluster size. This implies that the magnetocrystalline anisotropy for these smaller clusters is four times larger than that for bulk FCC cobalt and this is almost certainly due to distortions of the nanocrystal lattice. A second, and most important development is that it has been possible to make nanomaterials with a well-defined morphology, which can then be related to magnetic properties. Since this work has been carried out, we have developed methods of producing [22] intense beams of size-selected cobalt clusters and are therefore able to manufacture material with an even more carefully controlled morphology. This is an important step in the manufacture of novel materials whose properties can be related to their nanoscale structure.

### Acknowledgments

We would like to thank Daresbury Laboratory and the EPSRC for funding this research.

### References

- [1] Binns C 2001 Nanoclusters deposited on surfaces *Surf. Sci. Rep.* **44** 1
- [2] Mélinon P *et al* 1995 *Int. J. Mod. Phys. B* **9** 339
- [3] Yu Guoqing, Shi Ying, Chai Jianwei, Xie Dongzhu, Pan Haochang, Yang Guohua, Cao Jiangqing, Xu Hongjie and Zhu Dezhong 1998 *Nucl. Instrum. Methods B* **135** 382
- [4] Bromann K, Brune H, Felix C, Harbich W, Monot R, Buttet J and Kern K 1997 *Surf. Sci.* **377–9** 1051
- [5] Yoon B, Akulin V M, Cahuzac P, Carlier F, de Frutos M, Masson A, Mory C, Colliex C and Brechinac C 1999 *Surf. Sci.* **443** 76
- [6] Upwards M D, Cotier B N, Moriarty P, Beton P H, Baker S H, Binns C and Edmonds K 2000 *J. Vac. Sci. Technol. B* **18** 2646
- [7] Upwards M D, Moriarty P, Beton P H, Baker S H and Edmonds K 1997 *Appl. Phys. Lett.* **70** 2114
- [8] Bardotti L, Prével B, Treilleux M, Mélinon P and Perez A 2000 *Appl. Surf. Sci.* **164** 52
- [9] Tuillon J, Dupois V, Mélinon P, Prével B, Perez A, Pellarin M, Vialle J L and Broyer M 1997 *Phil. Mag. A* **76** 493
- [10] Eastham D A and Denby P M 2002 Formation of ordered assemblies from deposited gold cluster, at press
- [11] Perez A *et al* 1997 *J. Phys. D: Appl. Phys.* **30** 709
- [12] Eastham D A, Kirkman I W and Denby P M 2001 *Appl. Organom. Chem.* **15** 383  
Haberland H, Moseler M, Qiang Y, Rattunde O, Reiners T and Thurner Y 1996 *Surf. Rev. Lett.* **3** 887
- [13] Williams H D, O'Grady K and El-Hilo M 1993 *J. Magn. Magn. Mater.* **122**
- [14] Xiao G and Chien C L 1987 *J. Appl. Phys.* **61** 3308
- [15] Walker M, Mayo P L, O'Grady K, Charles S W and Chantrell R W 1993 *J. Phys.: Condens. Matter* **5** 2779  
Walker M, Mayo P L, O'Grady K, Charles S W and Chantrell R W 1993 *J. Phys.: Condens. Matter* **5** 2793
- [16] Néel L 1949 *Ann. Geophys.* **5** 99  
El-Hilo M, O'Grady K and Chantrell R W 1992 *J. Magn. Magn. Mater.* **117** 21
- [17] Aharoni A 1996 *Introduction to the Theory of Ferromagnetism* (Oxford: Clarendon) and references therein
- [18] Tischer M, Hjortstam O, Arvanitis D, Hunter Dunn J, May J F, Baberschke K, Trygg J, Wills J M, Johansson B and Eriksson O 1995 *Phys. Rev. Lett.* **75** 1602  
Tischer M, Hjortstam O, Arvanitis D, Hunter Dunn J, May J F, Baberschke K, Trygg J, Wills J M, Johansson B and Eriksson O 1995 *Phys. Rev. Lett.* **76** 1402
- [19] Eastham D A and Kirkman I W 2000 *J. Phys.: Condens. Matter* **12** L525
- [20] Fassbender J, Güntherodt G, Mathieu C, Hillebrands B, Jungblut R, Kohlhepp J, Johnson M T, Roberts D J and Gehring G A 1998 *Phys. Rev. B* **57** 5870  
Rodbell D S 1962 *J. Phys. Soc. Japan* **17** 313  
Doyle W D and Flanders P J 1965 *Proc. Phys. Soc. London* **86** 751
- [21] Weissmüller J 1996 *Nanomaterials: Synthesis, Properties and Applications* ed A S Edelstein and R C Cammarata (Bristol: Institute of Physics Publishing) ch 10, p 248 references therein
- [22] Denby P M and Eastham D A 2001 *Appl. Phys. Lett.* **79** 2477